

Late Jurassic lithological evolution and carbon-isotope stratigraphy of the western Tethys

Autor(en): **Padden, Maureen / Weissert, Helmut / Funk, Hanspeter**

Objektyp: **Article**

Zeitschrift: **Eclogae Geologicae Helvetiae**

Band (Jahr): **95 (2002)**

Heft 3

PDF erstellt am: **21.07.2024**

Persistenter Link: <https://doi.org/10.5169/seals-168964>

Nutzungsbedingungen

Die ETH-Bibliothek ist Anbieterin der digitalisierten Zeitschriften. Sie besitzt keine Urheberrechte an den Inhalten der Zeitschriften. Die Rechte liegen in der Regel bei den Herausgebern.

Die auf der Plattform e-periodica veröffentlichten Dokumente stehen für nicht-kommerzielle Zwecke in Lehre und Forschung sowie für die private Nutzung frei zur Verfügung. Einzelne Dateien oder Ausdrucke aus diesem Angebot können zusammen mit diesen Nutzungsbedingungen und den korrekten Herkunftsbezeichnungen weitergegeben werden.

Das Veröffentlichen von Bildern in Print- und Online-Publikationen ist nur mit vorheriger Genehmigung der Rechteinhaber erlaubt. Die systematische Speicherung von Teilen des elektronischen Angebots auf anderen Servern bedarf ebenfalls des schriftlichen Einverständnisses der Rechteinhaber.

Haftungsausschluss

Alle Angaben erfolgen ohne Gewähr für Vollständigkeit oder Richtigkeit. Es wird keine Haftung übernommen für Schäden durch die Verwendung von Informationen aus diesem Online-Angebot oder durch das Fehlen von Informationen. Dies gilt auch für Inhalte Dritter, die über dieses Angebot zugänglich sind.

Late Jurassic lithological evolution and carbon-isotope stratigraphy of the western Tethys

MAUREEN PADDEN, HELMUT WEISSERT, HANSPETER FUNK, STEFAN SCHNEIDER & CORNELIA GANSNER

Key words: Carbon-isotopes, Jurassic, Tethys, stratigraphy, paleoceanography

ABSTRACT

A new high-resolution carbon-isotope stratigraphy of the Late Jurassic has been generated from Tethyan carbonate sections. Sections chosen for this study are from the Helvetic nappes of the Swiss Alps, from the Jura Mountains, from the Provence (France) and from the Southern Alps (N. Italy). The limestones and marls used for this isotope geochemical investigation were deposited along the northern (Helvetic, Jura, Provence) and the southern (S. Alps) margin of the Alpine Tethys. Isotope curves were first established in well-dated sections of the Jura Mountains, the Southern Alps and the Vocontian Basin. Isotope curves generated from the poorly dated Helvetic nappe sections could then be correlated with the biostratigraphically dated sections.

This comparison produces greatly improved age control for the Helvetic sections and a more detailed composite $\delta^{13}\text{C}$ curve for the Late Jurassic than has been published previously. The composite $\delta^{13}\text{C}$ curve features two short-lived negative excursions in the Oxfordian, a $\delta^{13}\text{C}$ maximum in the Late Kimmeridgian and steadily decreasing $\delta^{13}\text{C}$ values throughout the Tithonian. These $\delta^{13}\text{C}$ events are consistent with previous, lower resolution data sets and are valuable tie-points, which can be used for correlating upper Jurassic successions among different lithologies and across different depositional settings. The new carbon isotope record is not only useful as a stratigraphic tool but it records fluctuations in Late Jurassic global carbon cycling. The negative carbon isotope events lasting up to a few 10^5 years are interpreted as primary perturbation signals recording anomalies in the atmospheric and marine carbon reservoirs. The perturbations of the global C-cycle were triggered by a sudden and massive release of methane stored in deep-sea gas hydrates. Positive carbon isotope excursions lasting up to millions of years record changes in carbonate and organic carbon production and sedimentation.

ZUSAMMENFASSUNG

Eine hochauflösende Kohlenstoff-Isotopenstratigraphie für den Späten Jura wurde in Karbonatprofilen des alpinen Raums gemessen. Die untersuchten Profile, die heute in den helvetischen Decken der Schweizer Alpen, im Jura-gebirge und in der Provence aufgeschlossen sind, entstammen dem Ablagerungsraum der nördlichen Tethys. Die Sedimente der Südalpen wurden am südlichen Tethysrand abgelagert. Als Ausgangspunkt für die Isotopenstratigraphie dienten biostratigraphisch gut datierte Profile des Juras, der Provence (Vocontischer Trog) und der Südalpen. Mit Hilfe der Isotopenstratigraphie konnten bisher schlecht datierte Profile des Helvetikums mit den gut datierten Abfolgen korreliert werden. Die neue Isotopenstratigraphie zeigt 2 kurzlebige negative Isotopenanomalien im Oxfordian (transversarium Zone, bifurcatus Zone). Eine positive C-Isotopenanomalie fällt in die pseudomutabilis Zone des späten Kimmeridgian. Die Untersuchungen bestätigen eine früher beobachtete kontinuierliche Abnahme der C-Isotopenwerte im Tithonian. Die Isotopenuntersuchungen haben bestätigt, dass die C-Isotopenstratigraphie zur Korrelation von lithologisch unterschiedlichen Gesteinsabfolgen aus Flachmeergebiet und Beckenmilieu verwendet werden kann. Die C-Isotopenkurve dient nicht nur zur stratigraphischen Korrelation, sondern zeichnet auch die Entwicklung des Kohlenstoffkreislaufs im Späten Jura auf. Die negativen C-Isotopenanomalien, die bis einige 10^5 Jahre gedauert hatten, werden als primäre Störsignale des C-Kreislaufs interpretiert. Die vermutlich eine plötzliche Destabilisierung von Gashydraten und damit massive Methanausbrüche anzeigen. Positive C-Isotopenanomalien, die bis zu Millionen von Jahren andauern, sind das Resultat von langfristigen Veränderungen in der Produktion und Sedimentation von organischem Material und von biogenen Karbonaten.

1. Introduction

Carbon isotope records of marine carbonate and organic matter can be used both as a stratigraphic and a paleoenvironmental tool (e.g. Arthur et al. 1985; Weissert 1989). In the present study $\delta^{13}\text{C}$ records are used primarily for stratigraphy. We generated a new carbon isotope stratigraphy for the Late Jurassic and we used the isotope stratigraphy to correlate

poorly dated lithological units with sections dated biostratigraphically. For our isotope study we sampled pelagic Upper Jurassic carbonate sections preserved in the Helvetic nappes of the Swiss Alps. These sections have been dated with a limited amount of biostratigraphic information (e.g. Rod 1937; Kugler 1987). In order to improve these age models, we compared the

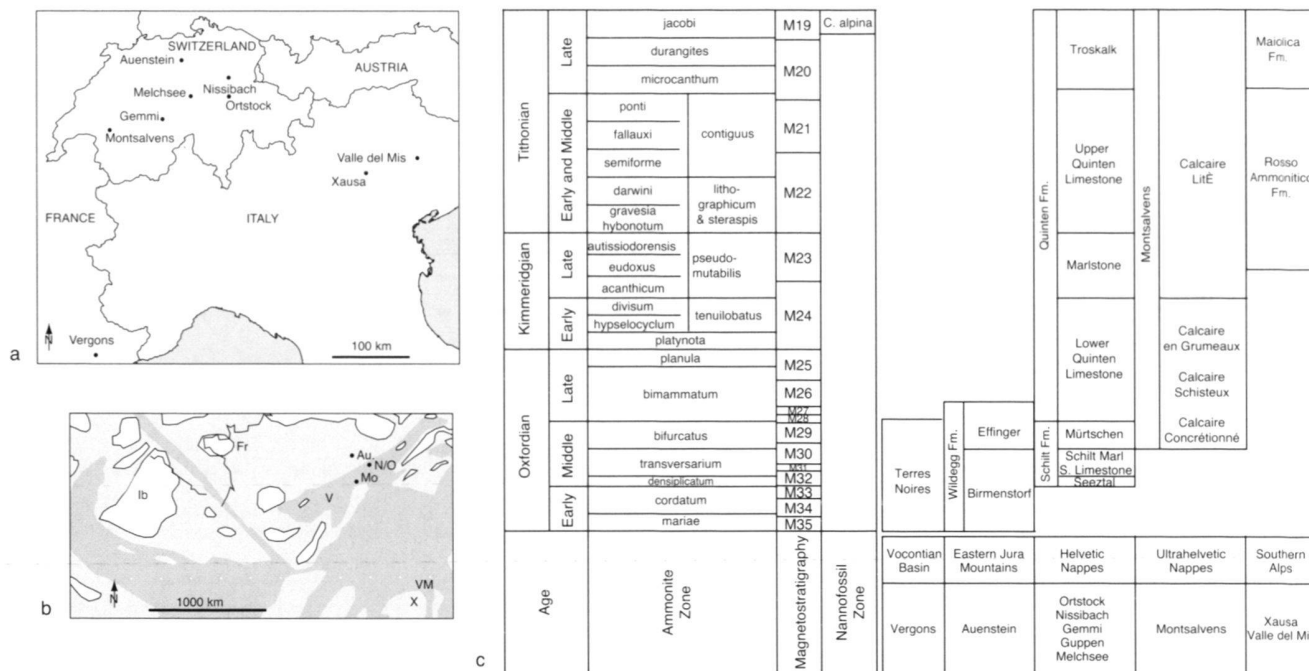


Fig. 1. Map a) shows present location of sites discussed in text. Map b) is a paleogeographic reconstruction (redrawn from Ziegler 1988) of the western Tethys Ocean. Dark grey areas are deep-marine settings, light grey areas are shallow-marine settings and white represents exposed land surfaces during the Late Jurassic. Ib indicates the Iberian Peninsula and Fr indicates France and the two black lines are an indication of modern coastlines of northern Spain and northwestern France. Figure c) presents lithological units discussed in text in a chronostratigraphic framework.

stable-isotope records of several Helvetic sections with biostratigraphically and, in some cases, magnetostratigraphically dated sections from the Jura Mountains of northern Switzerland, the Southern Alps of northern Italy and the Vocontian Basin of southeastern France. The new carbon-isotope stratigraphy is compared with carbon-isotope curves from extralpine terranes and it is used as a tracer of Late Jurassic changes in global carbon cycling.

2. The areas of Study

The areas of study are located in Switzerland in France and in Italy. One section is located in the Jura mountains of northern Switzerland, five sections are found in the Helvetic nappes of the Swiss Alps, another outcrops in the Ultrahelvetic nappes of western Switzerland and two southern Alpine sections are located in northern Italy (Fig. 1). The Jurassic sediments from the Jura Mountains and from the Helvetic nappes were deposited along the northern margin of the alpine Tethys. They represent a north-south transect from an inner platform to a basinal environment in the Alpine Tethys. For comparison, two sections deposited along the southern Tethyan margin as well as a section from the Vocontian Basin in southeastern France are also investigated. Samples were collected from sections where previous sedimentologic and chronostratigraphic work

had been done (e.g. Rod 1937; Guillaume 1957; Gygi & Persoz 1987; Kugler 1987; Weissert & Channell 1989; Mohr 1992; Schneider 1998; de Rafélis 2000; Gansner 2000).

3. Stable Isotope Geochemistry: Methods

Samples for stable isotope analysis were taken at intervals ranging from less than 10 cm to tens of meters and with a range of resolution from approximately 1 k.y to 2 My (Fig. 2–8). Fine-grained micrite samples were drilled with a diamond-tipped drill to produce a fine powder. This powder was reacted with phosphoric acid at 90 °C and the resulting CO₂ analyzed with a VG PRISM mass spectrometer following the standard procedure of Sharma & Clayton (1965). All isotope results are reported relative to the standard Vienna PeeDee Belemnite and measurement precision based on standards is better than ± 0.2 ‰. Relative abundances of total and inorganic carbon were measured on a UIC CM5012 Coulomat and expressed as wt % carbon. Organic-carbon abundance was calculated from the difference of these two measurements. Precision for carbonate carbon measurements is ± 0.1 ‰ for standards and ± 0.9 ‰ on natural samples, and organic carbon measurements have a precision of ± 0.1 ‰ measured on standards and ± 0.3% measured on natural samples. The precision of the calculated organic-carbon content is ± 0.14 based on standards and ± 0.95 based

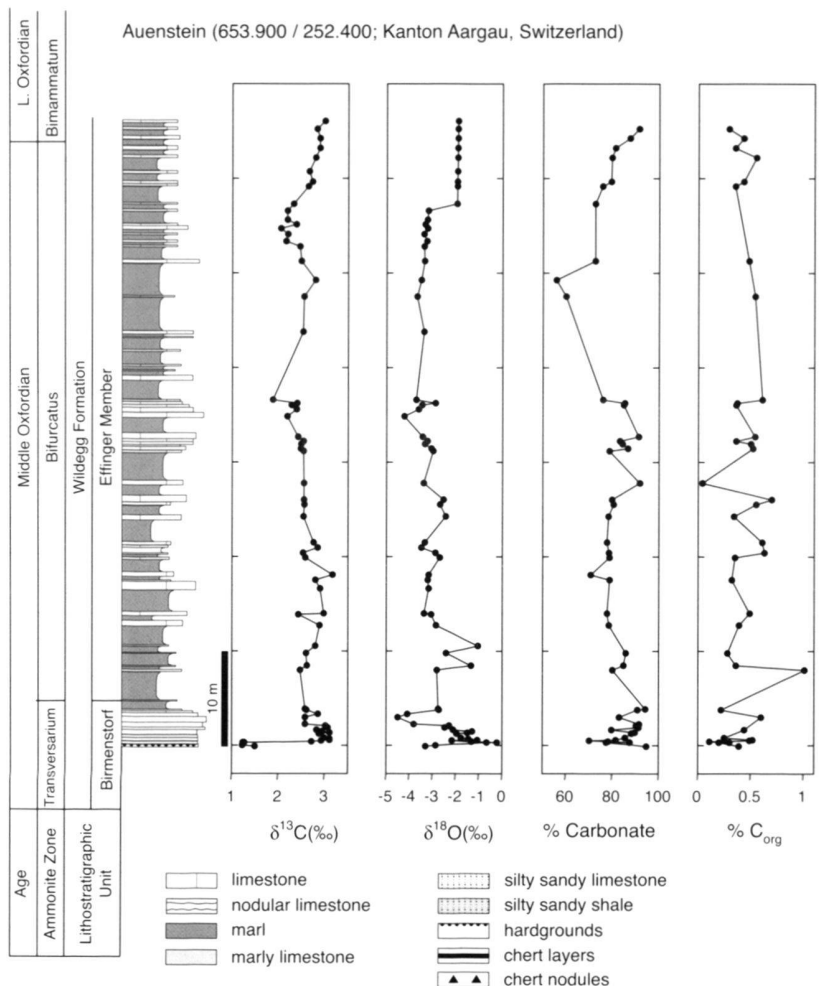


Fig. 2. Stratigraphy of the lowermost Wildegg Formation at Auenstein. Biostratigraphy after Gygi & Persoz (1987). Auenstein (653.900 / 252.400; Kanton Aargau, Switzerland)

on samples. For organic carbon-isotope analyses, samples were decarbonated with 37% HCl overnight. Organic carbon-isotope compositions and carbon and nitrogen abundance were measured on a Carlo Erba elemental analyzer coupled in continuous flow to a VG Optima mass spectrometer. The standard NBS 22 was used for organic isotopic analyses with a reproducibility of $\pm 0.3\text{‰}$. The elemental standard Atropina was used for carbon and nitrogen measurements with a reproducibility of $\pm 1.8\%$ for carbon and $\pm 0.06\%$ for nitrogen.

4. Site descriptions

4.1 Jura Mountains

The Jurassic sediments we used for our investigation are today outcropping in the Jura Mountains of northwestern Switzerland. They were deposited in a mixed carbonate-siliciclastic shallow epicontinental sea under warm subtropical conditions. The depositional area was divided into a platform region ("Celtic domain") and into a more basal environment ("Argovian domain"). The section "Auenstein" chosen for this in-

vestigation was part of the Argovian realm. The section (Fig. 2) crops out in a quarry in the eastern Jura fold belt, near the town of Wildegg and is the type section of the Wildegg Formation as defined by Gygi (1969). The sediments at Auenstein were deposited in an inner ramp environment along the northern Tethyan continental margin (Fig. 1; Gygi 1969; Gygi 2000a). The Early Oxfordian is represented by the Schellenbrücke Beds, a condensed horizon rich in glauconite (up to 2%) and also containing iron ooids (Kugler 1987). The Schellenbrücke Beds are overlain by the marls and limestones of the middle Oxfordian Wildegg Formation. The Wildegg Formation originally consisted of three members (Gygi 1969) but was later redefined to include only two members, the Birmenstorf Member and the Effingen Member (Gygi & Persoz 1987). The Birmenstorf Member consists of fossil-rich marls and limestones and it reaches a thickness of approximately 6 m at Auenstein. A rich macrofauna is preserved in the Birmenstorf Member including sponges (10–20%), ammonites, belemnites, echinoderms (crinoids and echinoids) and brachiopods (terebratulids and rhynchonellids). Carbonate content in the Birmenstorf Member ranges from 60 to 97% and organic carbon

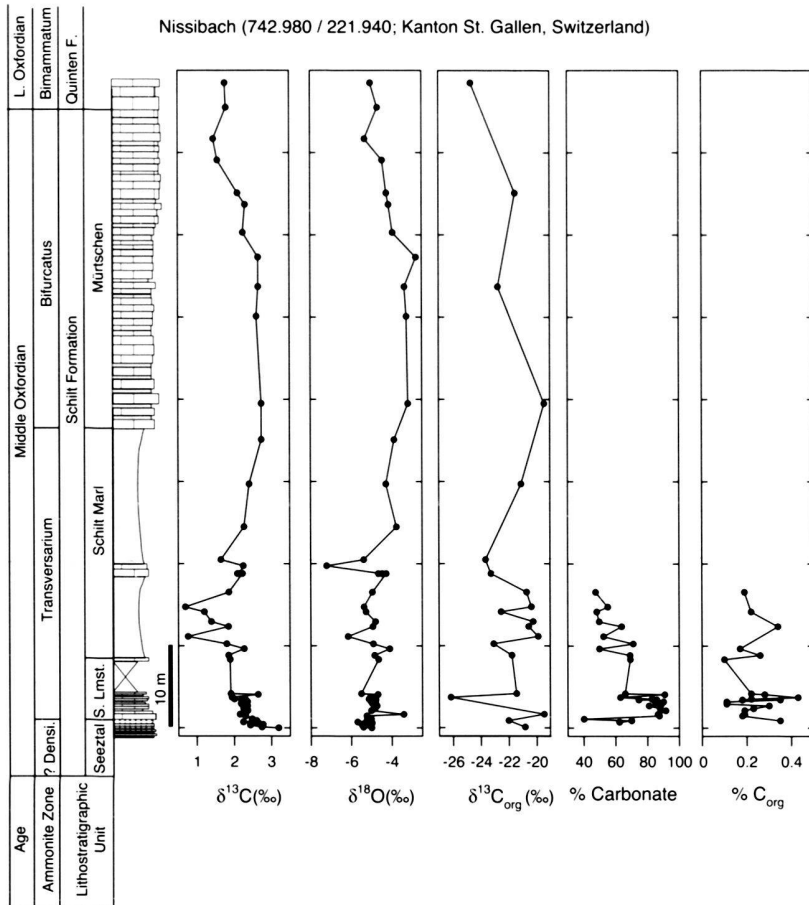


Fig. 3. Stratigraphy of the Schilt Formation at Nissibach. For lithological legend, see Fig. 2.

(Corg) is less than 1% (Fig. 2). The overlying Effingen Member consists of 210 m of interbedded marls and limestone beds; the limestone beds in the lowermost 20 m are laterally discontinuous at this site (Fig. 2). Most limestone beds are 10 to 20 cm thick with some beds reaching thicknesses of 70 cm. Fossiliferous horizons in the lower Effingen Member contain ammonites, sponges, belemnites, brachiopods and echinoderms.

The Late Jurassic carbonate sequences outcropping in the Jura Mountains of northern Switzerland have been studied extensively and this paper cannot do justice to the entire literature. Gygi (2000a) provides a useful summary of the Late Jurassic chronostratigraphic framework of this region. Ammonite chronology (Gygi & Persoz 1987; Gygi 2000b) produces a robust correlation of the Birmenstorf and Effingen members of the Wildegg Formation throughout northeastern Switzerland. Sedimentation and paleotectonic evolution of the Oxfordian basins of northern Switzerland have recently been investigated by Allenbach (2001). The time scale of Gradstein & Ogg (1996) is used to assign radiometric ages to ammonite zones and magnetostratigraphic zones. Isotopic samples were collected from the Birmenstorf Member and from limestone beds in the lowermost 60 m of the Effingen Member.

4.2 Helvetic Nappes

Schilt Formation

Nissibach and Ortstock are located in the Gonzen Nappe and the Axen Nappe respectively which belong, tectonically, to the Helvetic nappes of the Swiss Alps (Kugler 1987). The Schilt Formation (Middle to Late Oxfordian), outcropping at Nissibach (Fig. 3) and Ortstock (Fig. 4), represents a time-equivalent to the Wildegg Formation. A detailed examination of the sedimentary and faunal characteristics of the Schilt Formation and comparison to the Wildegg Formation is described in Kugler (1987). The Schilt Formation represents an outer ramp paleoenvironment along the northern Tethyan continental margin (Fig. 1). Based on the descriptions of Kugler (1987), we divide the Schilt Formation into four members: Seetzal Member (Mb.), Schilt Limestone Mb., Schilt Marl Mb. and Mürtschen Mb.

The Seetzal Member is 3 m thick at Nissibach and 15 m thick at Ortstock and is composed of silty and sandy shales with carbonate content < 35% and detrital quartz abundance between 20 and 40%. Organic-carbon content is <1% through-

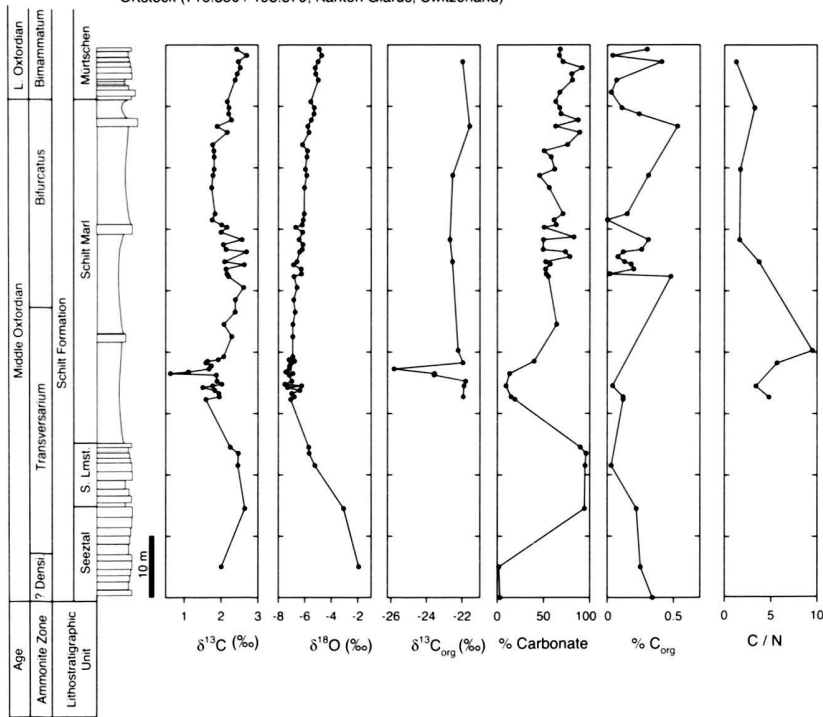


Fig. 4. Stratigraphy of the Schilt Formation at Ortstock. For lithological legend see Fig. 2.

out the entire Schilt Fm. Bioturbation is present in the Seetzal Member and phosphate nodules are frequently associated with ammonites. Quartz abundance decreases towards the contact with the Schilt Limestone Member. At Nissibach and Ortstock, the upper part of the Seetzal Member becomes increasingly calcareous and contains chamositic Fe ooids and echinoderm spines.

The Schilt Limestone member is 8 m thick at Nissibach and 10 m at Ortstock. This micritic, bioturbated and locally nodular limestone succession contains minor amounts of dolomite and is virtually free of detrital material. Non-dolomitized limestone is dark grey, micritic, and weathers to a light grey colour. The Schilt Limestone member contains a rich, though poorly preserved cephalopod fauna which can form calcareous nodules in a marly matrix. Echinoderm remains are also present in this member.

The Schilt Marl Member is extensive at both Nissibach and Ortstock (27 and 55m respectively) and features dark grey marls with carbonate content between 35 and 75% as well as isolated beds of dark, micritic limestone (Figs. 3 and 4). This member contains few fossils and no coarse detrital material. Small calcareous nodules in a marly matrix can be seen in the basal layers of the Schilt Marl member at Nissibach and in the uppermost Schilt Marl at Ortstock.

The Mürtschen Member consists of well-bedded, grey limestones interbedded with marls and is 42 m thick at Nissibach and 8m thick at Ortstock. Bedding is irregular and individual beds are between 15 and 35 cm thick. Fossils and detri-

tal matter are both absent in the limestone beds. Small, dark, calcareous nodules are present in both the limestone and marl beds. There is a gradual transition to the overlying Quinten Formation as the limestone beds become more frequent and interbedded marls become thinner. Kugler (1987) defined the contact between the Mürtschen Member and the Quinten Formation to be where the marly interbeds of the Mürtschen Member are reduced to less than 2 cm thickness.

Several nodular limestone beds occur in the studied sections. In the Schilt Limestone and Mürtschen Members, nodules are commonly associated with ammonite moulds or are irregular in shape. Nodules range in size from 0.5mm – 2cm and are randomly oriented and unsorted in a micritic to microsparitic and slightly marly matrix. The nodules are composed of tightly packed, uniform micrite which is usually about 2 μ in size. There is no sparite present in the nodules and nodules with diffuse and clear boundaries may occur in the same sample. The boundary is often much easier to see macroscopically than microscopically.

The Seetzal, Schilt Limestone and Schilt Marl members are dated by ammonite stratigraphy (Kugler 1987). The Seetzal Mb. spans the Lamberti zone of the late Callovian to the Den-siplicatum zone of the middle Oxfordian (Kugler 1987). The Schilt Limestone Mb. and Schilt Marl Mb. cover the Transversarium zone and perhaps part of the Bifurcatus zone; however the boundary between the Schilt Marl and the Mürtschen Mb. is poorly dated due to lack of fossils (Kugler 1987). The Mürtschen Mb. itself is fossil-poor throughout and therefore

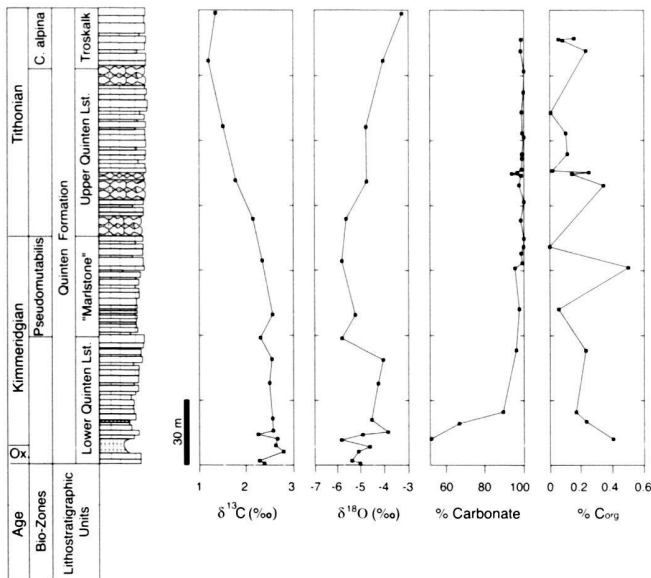


Fig. 5. Stratigraphy of the Quinten Formation at Gemmi. For lithological legend, see Fig. 2.

difficult to date with biostratigraphic methods. A minimum age is provided by the presence of *Epipeltoceras Bimammatum* in the overlying Quinten Formation (Kugler 1987; see below).

Quinten Formation

Previous sedimentological observations and isotopic analyses of the Quinten Formation are reported from other sites in the Helvetic nappes at Guppen-Heuberg (Mohr 1992; Funk et al. 1993; Weissert and Mohr 1996), Melchsee (Schneider 1998) and Gemmi (Gansner 2000; Fig. 5). The lowermost 160 m of the Quinten Formation crop out at Melchsee and the entire formation can be observed at Guppen-Heuberg (415 m) and Gemmi (210 m). The Quinten Formation is divided by most authors into the Lower Quinten Limestone (LQL), the Marlstone Member (MM), Upper Quinten Limestone (UQL) and the Troskalk Member (e.g. Rod 1937; Mohr 1992). The lowermost Quinten Limestone is a series of regularly-bedded (20–50 cm), dark grey, micritic limestones with low (<1%) organic content. Bedding becomes indistinct towards the contact to the Marlstone Member at Gemmi and Guppen (Mohr 1992; Gansner 2000). Carbonate content ranges from 93–100% and nodular limestones are present in the Lower Quinten Limestone at Guppen (Mohr 1992). There is significant dolomitization associated with these nodules (Mohr 1992) whereas dolomite appears in the Upper Quinten Limestone at Gemmi (Gansner 2000) and is completely absent in the Quinten Formation at Melchsee. Horizons with abundant belemnite and

ammonite remains occur in the Lower Quinten Limestone at Melchsee (Schneider 1998). At Guppen-Heuberg, dolomitized or silicified belemnites, ammonites, bivalves and echinoderm fragments also occur along isolated horizons (Mohr 1992). The Lower Quinten Limestone at Gemmi appears to be relatively fossil-poor (Gansner 2000).

The Lower Quinten Formation at Melchsee contains nodular limestones which can be classified into two different types according to colour. The first type which occurs just above the Schilt Formation displays predominantly ammonite nodules which are usually about 0.5 to 2 cm in diameter although some reach sizes of 7cm. These round to oval nodules are filled with light-coloured micrite. There is usually a sharp boundary between the nodule and the matrix although there are some examples of diffuse boundaries. Once again, the boundary between nodule and matrix is difficult to distinguish under the light microscope. This type of nodular limestone grades into the next type containing less well-rounded, dark grey nodules which do not appear to be predominantly associated with ammonite moulds.

The Marlstone Member of the Quinten Formation contains marl at Guppen-Heuberg (Mohr 1992; Weissert & Mohr 1996) but no marls at either Gemmi or Melchsee. At Guppen-Heuberg, this member consists of fossil-poor, thin-bedded (10–20 cm) dark grey micritic limestones interbedded with 2 cm thick dark grey marls (Mohr 1992). At Gemmi, the Marlstone Member contains 10% bioclasts including belemnites, bivalves, echinoderms ammonites and *Saccocoma* and 2% silt-sized quartz. Chert nodules and minor amounts of dolomite and pyrite are also present. A thinbedded (5–10 cm), fossil-poor unit forms the Marlstone Member at Melchsee.

Dolomitized nodules reappear in the Upper Quinten Limestone member at Guppen (Mohr 1992) and are especially common along fossil-rich horizons. At Gemmi, nodular intervals often take the form of a 'pseudobreccia' which consists of dark nodules in a light grey matrix. The Upper Quinten Limestone is only partially preserved at Melchsee and consists of thin (3–10 cm) micritic beds. Bed-parallel chert bands are also present in the Upper Quinten Limestone at Guppen and continue throughout the uppermost Troskalk member (Mohr 1992).

The Troskalk Member, present at Gemmi and Guppen, is a thick-bedded (~1m) unit rich in platform-derived fossil remains (Mohr 1992; Funk et al. 1993). Faunal elements represent up to 19% of the limestone and include echinoderms, bivalves, benthic foraminifera, gastropods, bryozoa, brachiopods and serpulids (Mohr 1992). Fist-sized coral fragments were also found at Guppen (Mohr 1992; Funk et al. 1993).

Ammonites representing the *Bimammatum* Zone are found in the Lower Quinten Limestone (Kugler 1987). The Marlstone Member, also dated by ammonite stratigraphy, occurs in the *Pseudomutabilis* zone of the Late Kimmeridgian (Rod 1937). The age control for the Late Tithonian Upper Quinten Limestone is provided by calpionellids (Mohr 1992).

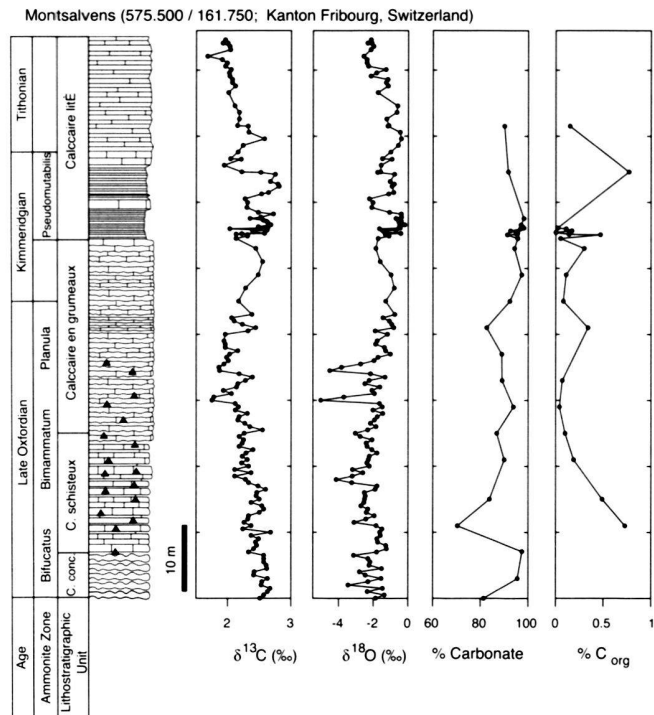


Fig. 6. Stratigraphy of the Late Jurassic succession at Montsalvens. For lithological legend, see Fig. 2.

4.3 Ultrahelvetica Nappes

The Montsalvens section (Fig. 6) is located in the Ultrahelvetica nappes of western Switzerland (Fig. 1). The carbonate sequence outcropping at the Montsalvens Gorge along the Jogne river was studied in great detail by Guillaume (1957) and divided into four lithological units: Calcaire concrétionné, Calcaire schisteux, Calcaire en grumeaux and Calcaire lité.

Calcaire concrétionné refers to a series of alternating 5–10 cm nodular marls and 15–20 cm thick micritic limestones. At the Montsalvens site, 7 m of Calcaire concrétionné is exposed. Nodules are dark grey, calcareous and are commonly associated with ammonites (Guillaume 1957). Carbonate content of the limestones ranges from 80 to 100% (Fig. 6). Organic carbon constitutes less than 1% throughout the Montsalvens section.

The abrupt disappearance of interbedded marls signals the contact to the Calcaire schisteux, an 18 m series of regularly bedded dark grey micritic limestones (Guillaume 1957). Bedding ranges from 10–40 cm and siliceous nodules are locally isolated and can occur as narrow (<10 cm) bands. Carbonate content ranges between 65–94% and preserved fossils are rare.

A switch to wavy bedding marks the transition to the Calcaire en grumeaux. The name is related to the French word for

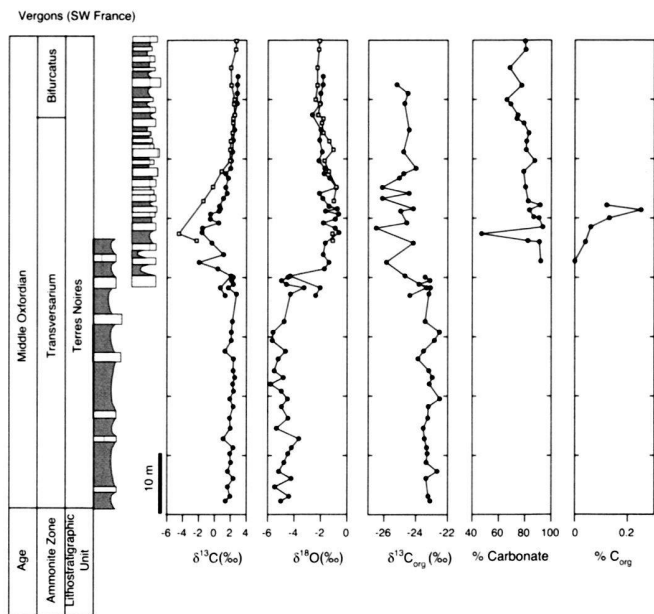


Fig. 7. Stratigraphy of the uppermost Terres Noires succession at Vergons. Squares represent data from de Rafelis (2000). Carbonate content and biostratigraphy are from de Rafelis (2000). For lithological legend, see Fig. 2.

curled and refers to the occasionally mottled appearance of these limestones due to calcareous and siliceous nodules forming irregular ovoids in a micritic matrix. The limestones contain 80–96% CaCO₃ with less chert than the Calcaire schisteux. Bedding is generally 5–15 cm thick although some beds reach thicknesses of 40–50 cm. An 8 m series of very finely bedded (<10cm) micritic limestones forms the base of the Calcaire lité. Bedding thickness in the upper part of the Calcaire lité averages 10 cm. These regularly bedded limestones contain 87–94% CaCO₃ with no discernible chert. Belemnite and ammonite aptychi remains are rare, although some ammonites are found at the base of the Calcaire lité (Guillaume 1957).

At Montsalvens, there are nodular levels in the Calcaire concrétionné and in the Calcaire en grumeaux (Guillaume 1957). The main difference between the two members is the presence of marl in the Calcaire concrétionné. The calcareous nodules tend to be dark grey, irregular ovoids and, in the Calcaire concrétionné, are commonly associated with ammonite molds (Guillaume 1957).

Based on ammonite associations and lithological comparisons to the Quinten Formation, Guillaume (1957) provided the following age estimates for the limestone succession at Montsalvens: The Calcaire concrétionné was estimated to be of middle Oxfordian age, the Calcaire schisteux and Calcaire en grumeaux of late Oxfordian to early Kimmeridgian age and the Calcaire lité of Kimmeridgian to early Tithonian age.

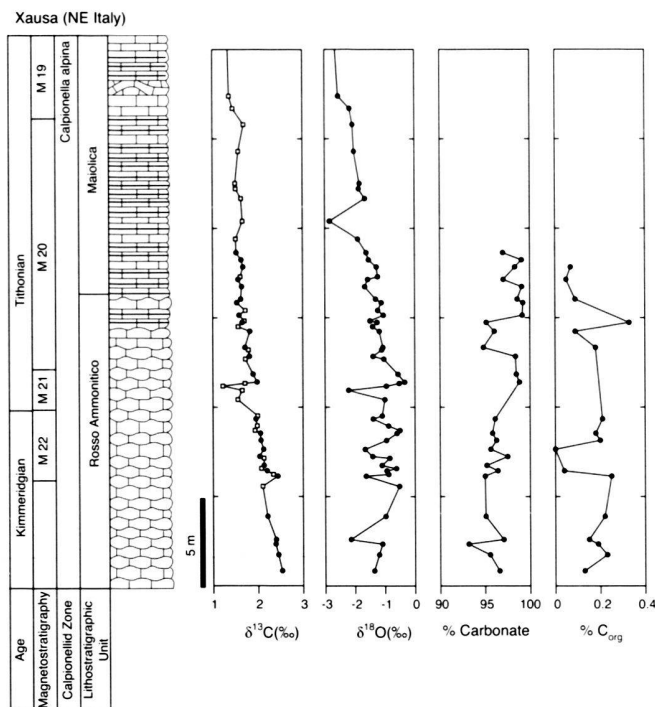


Fig. 8. Stratigraphy of the Rosso Ammonitico - Maiolica transition at Xausa. Squares represent data from Weissert and Channell (1989). Magnetostratigraphy and biostratigraphy after Weissert & Channell (1989). For lithological legend, see Fig. 2.

4.4 Vocontian Basin

A 150 m section of the upper Terres Noires outcrops near the town of Vergons in southeastern France (Fig. 7). Sequence stratigraphic work at this site incorporated lithology, trace-element (Mn, Sr) analyses, palynological data and isotopic analysis (de Rafelis 2000; Jan du Chene et al. 2000). For the present study, the Vergons section was resampled at a higher resolution and sampling was extended down the section. Both isotopic records are shown in figure 7. In the lower part of the section, dark grey marly limestones, 10–40 cm thick, are interbedded with dark grey marls reaching thicknesses of 150 cm. Limestones become more frequent and the marly intervals thinner upwards in the section (Fig. 7). Carbonate content of the upper portion ranges between 66 and 97%. Organic carbon was measured on five samples; it is less than 0.25%. Preserved fauna include belemnites and ammonites (Jan du Chene et al. 2000; pers. obs.). Grainstones with well-rounded bioclasts and slump deposits are common above the sampled section where marl beds disappear completely (Jan du Chene et al. 2000).

The Vergons section is dated by ammonites, dinoflagellates and sequence stratigraphy (Jan du Chene et al. 2000). The Transversarium/Bifurcatus transition is present in the upper part of the section; however, the lower Transversarium/Densi-

plicatum transition was not found at this site. We assume, therefore, that the lower part of the section lies within the Transversarium zone.

4.5 Southern Alps

Isotopic data from two southern Alpine sections, Valle del Mis located in the Belluno Basin and Xausa located on the Trento Plateau, are reported in Weissert & Channell (1989). The 60 m Tithonian/Berriasian section at Valle del Mis was first described by Casati & Tomai (1969) and Weissert (1979) and contains the transition from the Rosso Ammonitico Superiore to the Maiolica Formation. At this location, the Rosso Ammonitico Superiore is a red-gray nodular marly limestone. Chert occurs as reddish-brown nodules and bands. The overlying Maiolica Formation consists of white to grey thin-bedded (5–40 cm) limestones interbedded with siliceous marls. Evidence of sporadic redeposition includes sorting of pelagic bivalves, current lamination and, rarely, carbonate turbidites (Weissert & Channell 1989).

The same formations are also present at Xausa (Fig. 8). The 15m exposure of the Rosso Ammonitico Superiore displays a reddish nodular limestone with marly interbedding. Towards the contact with the Maiolica Formation, there is a gradual decrease in nodularity and a colour shift from red to alternating pink and white limestone beds. The 50 m Maiolica Formation at this site is similar to that of Valle del Mis although evidence of resedimentation is lacking. Faunal elements present in the limestone beds of the Maiolica Formation include coccoliths and nannoconids, calpionellids, calcispheres, radiolarians and ammonite aptychi (Weissert 1979). Isotopic data from the Xausa section, presented in Weissert & Channell (1989), has been augmented for the present study (Fig. 8). The Rosso Ammonitico Superiore was sampled at a higher resolution and the record extended to a lower stratigraphic level (Fig. 8).

A combination of magnetostratigraphy and nannofossil analysis constrains the age of the section at Xausa and Valle del Mis (Channell et al. 1987; Channell & Grandesso 1987; Weissert & Channell 1989). The Tithonian is represented by magnetic anomalies M19 through M22 and the *Calpionella alpina* zone (Fig. 8). A summary of the correlation of magnetostratigraphy and nannofossil zones with ammonite zones is given in Gradstein & Ogg (1996; Fig. 1).

5. Stable-Isotope Results

5.1 Carbon

The presented bulk carbonate $\delta^{13}\text{C}$ data fluctuate between 0.3 and 3.3‰ (Figs. 9–11). There is a negative excursion, of 2 to 6‰ in magnitude, which is dated as Transversarium age at Auenstein (Gygi & Persoz 1987) and Vergons (de Rafelis 2000; Fig. 9). A second, more subdued (< 1‰ in magnitude) negative excursion is dated at Auenstein to occur in the Bifur-

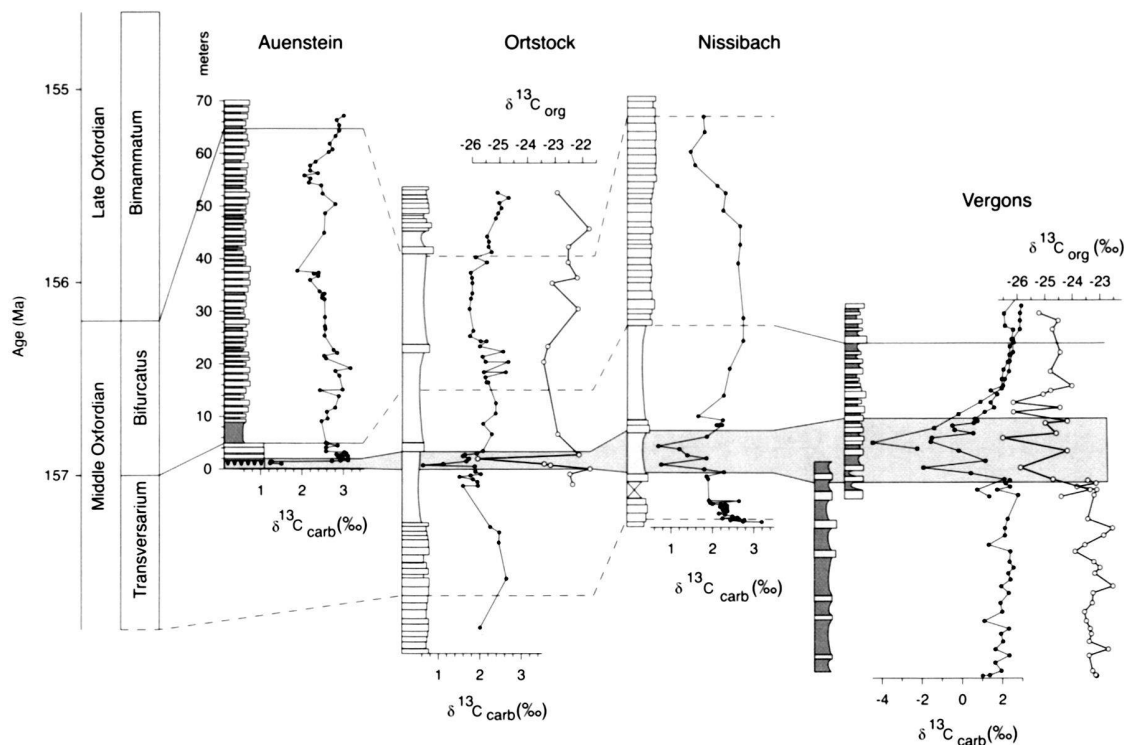


Fig. 9. Summary of correlation of Oxfordian $\delta^{13}\text{C}$ records. All sections are plotted vs. the meter scale to the left of the Auenstein data. Solid-line correlations indicate index fossils were found at location. Dashed-line correlations are based on regional lithostratigraphic correlations by Kugler (1987) and isotopic correlations. The open circles in the Ortstock and Vergons profiles represent $\delta^{13}\text{C}_{\text{org}}$ data. Filled squares in the Vergons profile are from de Rafelis (2000) and filled circles are from the present study. For lithological legend, see Fig. 2.

catus zone (Gygi & Persoz, 1987). The composite carbon isotope curve then rises steadily and reaches a maximum of about 3‰ in the Late Kimmeridgian (Fig. 10), dated at Guppen and Melchsee according to Rod (1937). There is a steady decrease in $\delta^{13}\text{C}$ values throughout the Tithonian, an interval dated at Xausa and Valle del Mis (Weissert & Channell 1989). The carbonate $\delta^{13}\text{C}$ record reaches values of approximately 1.5‰ at the Jurassic/Cretaceous boundary.

Organic carbon $\delta^{13}\text{C}$ ($\delta^{13}\text{C}_{\text{org}}$) data measured at Ortstock and Vergons range from -26.5 to -21.5‰ (fig. 9). A negative $\delta^{13}\text{C}$ excursion, of 2 to 3‰ in magnitude, coincides with the Transversarium excursion in the carbonate records at both sites (Padden et al. 2001).

5.2 Oxygen

The oxygen isotope data presented here range between -7.2 and 0.7‰. In addition to a much higher range of values, the oxygen isotope data display very poor agreement between sections. The most negative $\delta^{18}\text{O}$ values occur at Nissibach and Ortstock, intermediate values occur at Gemmi, Guppen and Melchsee and the most enriched $\delta^{18}\text{O}$ values in the sections at

Auenstein, Montsalvens, Xausa and Vergons. The marly sediments at Nissibach, Ortstock and in the lowermost Vergons section also display relatively depleted $\delta^{18}\text{O}$ values. There is no consistent stratigraphic trend in the $\delta^{18}\text{O}$ data among the sections.

6. Discussion

6.1 Diagenesis

Many studies have demonstrated the value of carbon isotopes as a stratigraphic tool in carbonate successions (e.g. Scholle & Arthur 1980; Weissert & Lini 1991; Jenkyns et al. 1994; Jenkyns 1996; Ferreri et al. 1997; Menegatti et al. 1998 and many others). In Alpine settings, carbon isotopes are much less susceptible than oxygen isotopes to resetting during recrystallization at high burial temperatures (e.g. Matter et al. 1975). A comparison of different Late Jurassic $\delta^{13}\text{C}$ records shows an excellent correlation across depositional environments and lithologies (Fig. 2-8; Fig. 11). The good correlation between nodular and non-nodular sediments in the carbon-isotope record (Fig. 11) indicates that the effect of nodule forma-

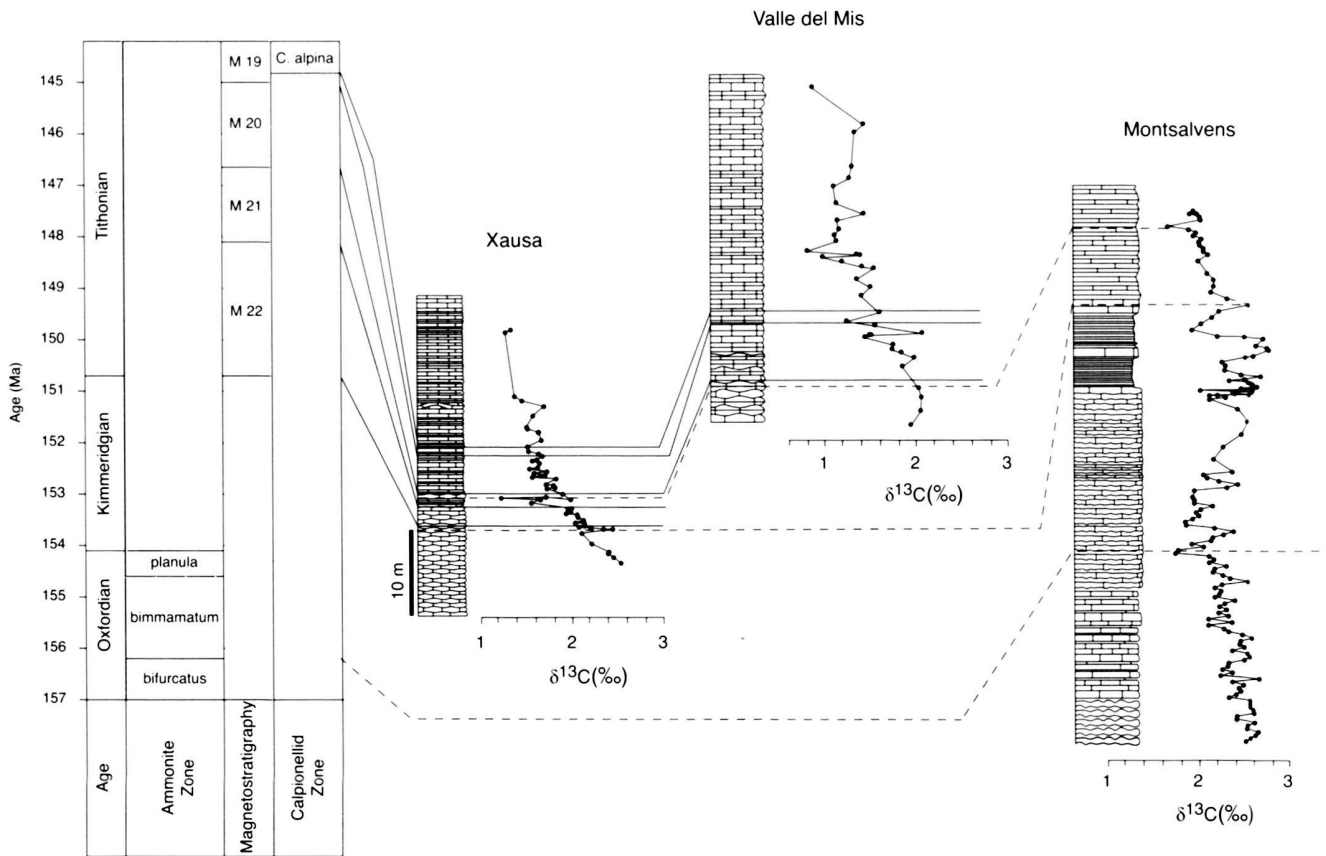


Fig. 10. Summary of correlation of Kimmeridgian-Tithonian $\delta^{13}\text{C}$ records. Dashed line represents $\delta^{13}\text{C}$ correlations. Solid line based on magnetostratigraphic measurements and calpionellids found at Xausa and Valle del Mis.

tion appears to have had little or no impact on the isotope record. In a similar way, dolomitization does not appear to have adversely affected the carbon isotope records since the dolomitized and non-dolomitized sections correlate very well (Fig. 11). The generally good agreement between the presented data and previous records by Jenkyns (1996) and especially the $\delta^{13}\text{C}$ record from a series of cherty limestones by Bartolini et al. (1999) confirms the robustness of the presented carbon-isotope signal among different lithologies. The very low organic-carbon content of the samples also reduces the likelihood of postdepositional exchange of carbon atoms (Fig. 2–8). The application of carbon-isotope stratigraphy in condensed sediments is justified by the preservation of the Oxfordian negative excursion in the series of condensed beds at Auenstein.

Oxygen isotopes, on the other hand, are subject to re-equilibration with interstitial water at high burial temperatures and tend to become more depleted than the original value (e.g. Fröh-Green et al. 1990). The robustness of the $\delta^{13}\text{C}$ signal in the studied sections is supported by the overlapping curves of the 7 different sections which have been subject to different

degrees of metamorphism and whose $\delta^{18}\text{O}$ curves show an expected negative offset with increasing burial temperature (Fig. 12).

The oxygen-isotope values of cherty limestones also show a tendency towards negative values. More detailed study is called for, but a speculative explanation of this phenomenon is the exchange of oxygen atoms between SiO_2 , CaCO_3 and a fluid phase during chert nodule formation. This effect can be seen in the Montsalvens data where anomalously negative $\delta^{18}\text{O}$ values occur in chert-rich intervals (Fig. 6). The $\delta^{18}\text{O}$ values from the cherty limestones of the Appenines (Bartolini et al. 1999), are also relatively negative although the depth of tectonic burial is equal to or less extreme than at Montsalvens or in the Helvetic nappes. The potential effect of marly sedimentation on $\delta^{18}\text{O}$ values is best illustrated in the Vergons section. The lower part of the section is very marly and shows the most depleted $\delta^{18}\text{O}$ values. Depleted $\delta^{18}\text{O}$ carb values at Nissibach and Ortstock may be due to the marly lithology as well as recrystallization during burial. Therefore oxygen isotopes may be compromised in cherty carbonates and marls even when carbon-isotope signals appear to be preserved.

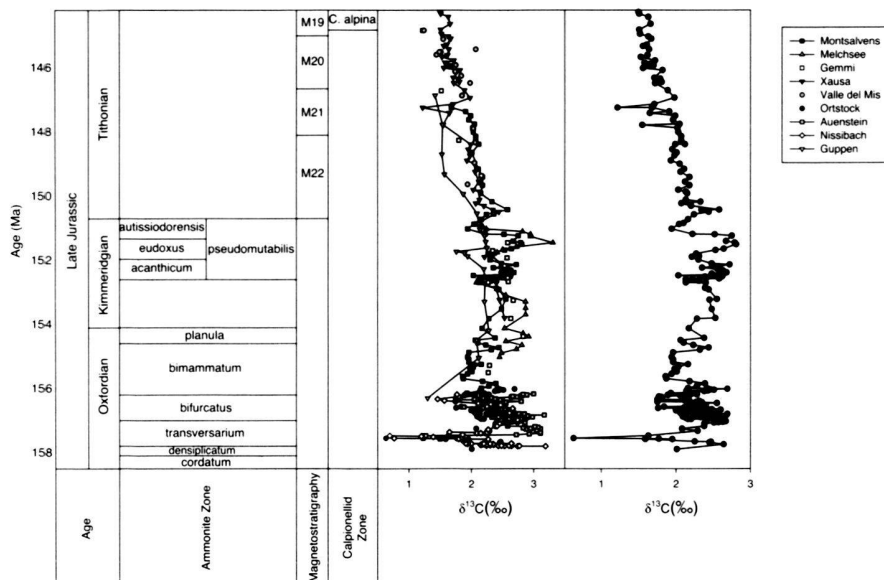


Fig. 11. $\delta^{13}\text{C}$ curves vs. age. Composite $\delta^{13}\text{C}$ curve on the right is composed of Ortstock, Montsalvens and Xausa

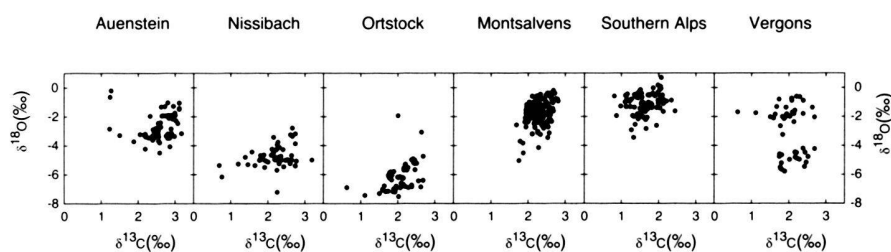


Fig. 12. Crossplots of $\delta^{13}\text{C}$ vs $\delta^{18}\text{O}$ data. The most negative $\delta^{18}\text{O}$ values occur at Nissibach and Ortstock, pointing to significant burial and recrystallization in the Helvetic nappes.

6.2 Carbon-Isotope Stratigraphy

Carbon-isotope stratigraphy is an excellent tool to fine-tune platform-basin correlations because many studies have shown that original carbon-isotope values are preserved even after tectonic burial (Früh-Green 1998) and peri-platform sediments have the same isotopic compositions as coeval pelagic sediments (e.g. Wissler et al. 1999). In the present data set, the distinct $\delta^{13}\text{C}$ fluctuations are subtle, which allows for a detailed correlation among the sections sampled at a high resolution (Fig. 11) and a more speculative correlation of lower resolution data.

The Transversarium negative $\delta^{13}\text{C}$ excursion is present in four sections: Auenstein, Nissibach, Ortstock and Vergons. This isotopic signature is securely dated in the Birmenstorf Mb. at Auenstein and at Vergons and corroborates the chronological scheme proposed by Kugler (1987) for the Schilt Marl Mb. of the Schilt Fm. at Ortstock and Nissibach. Negative $\delta^{13}\text{C}$ shifts of similar magnitude have also been reported for Transversarium-aged limestones in the western Jura Mountains (Bill et al. 1995) and in mid-Oxfordian sediments in the

Gulf of Mexico (Humphrey et al. 1986). This corroboration supports the contention that carbon isotopes record a global signal (Padden et al. 2001).

The Bifurcatus negative excursion is present in the Effingen Mb. at Auenstein, in the Schilt Marl Mb. at Ortstock, in the Mürtchen Mb. at Nissibach and in the Calcaire en grumeaux at Montsalvens. This excursion is well dated only in the Effingen Mb. at Auenstein, but the time-frame is consistent with chronologies proposed for the Helvetic sections (Kugler 1989) and Montsalvens (Guillaume 1957) based on biostratigraphy. The positive Late Oxfordian $\delta^{13}\text{C}$ values which occur between the two negative excursions have also been reported from sediments in northern Italy and southern France by Jenkyns (1996) and in the Southern Alps by Bartolini et al. (1999). The $\delta^{13}\text{C}$ maximum in the late Kimmeridgian (Pseudomutabilis zone) is well-dated in the Marlstone Member of the Quinten Fm. at Guppen (Weissert & Mohr 1996), Gemmi and Melchsee (Rod 1937) and can be correlated to the Calcaire lité at Montsalvens (Fig. 11). A positive $\delta^{13}\text{C}$ excursion in the Late Kimmeridgian has also been found in the North Atlantic by

Scholle & Arthur (1980) and in the Southern Alps by Bartolini et al. (1999). No biostratigraphic control is available between the negative $\delta^{13}\text{C}$ excursion in the Bifurcatus zone and the late Kimmeridgian $\delta^{13}\text{C}$ maximum in the Pseudomutabilis zone, therefore a constant sedimentation rate must be assumed between these two control points.

The Tithonian trend towards more depleted $\delta^{13}\text{C}$ values, dated by magneto- and biostratigraphy at Xausa and Valle del Mis (Weissert and Channell 1989), can be correlated with a similar trend at Montsalvens providing age control for the Montsalvens section during the Tithonian (Fig. 11). The trend toward more depleted $\delta^{13}\text{C}$ values throughout the Tithonian has also been documented by Letolle et al. (1978), Scholle & Arthur (1980) and Weissert & Channell (1989).

The overall agreement between the Late Jurassic carbon-isotope stratigraphy described in this study and that of previous authors confirms that $\delta^{13}\text{C}$ stratigraphy is a valuable stratigraphic tool with potential for resolving relatively fine-scaled stratigraphic problems. However, high resolution sampling is needed when correlating a carbon-isotope record as subtle as that of the Late Jurassic.

6.3. Carbon-Isotope Stratigraphy and Carbon Cycle

If the ratio of ^{13}C to ^{12}C in carbonates and in organic matter reflects an original, marine composition then it can be used as a proxy for paleoceanography and as tracer of the global carbon cycle. On long time scales of 10^4 to 10^7 years, variations in the C-isotope composition of sedimentary organic and carbonate carbon can be interpreted as the result of changes in organic and/or carbonate carbon flux from the ocean into the sedimentary carbon sink. At times of high organic carbon burial rates carbon-13 became enriched in the ocean water. This change in past oceanic isotope signature is stored as a positive carbon isotope anomaly in the rock record. We identified two episodes with elevated $\delta^{13}\text{C}$ -values in the Late Jurassic carbon isotope curve. The first one is dated as Late Oxfordian, the second one falls into the Late Kimmeridgian (pseudomutabilis zone). If compared with the prominent carbon isotope anomalies in the Valanginian and Aptian (Weissert et al., 1998) the late Jurassic positive carbon isotope events are smaller in amplitude and shorter in duration. This suggests that perturbations of Late Jurassic carbon cycling were less extreme than in the Cretaceous. In addition, high organic carbon burial rates were buffered by high carbonate carbon burial rates during the Late Jurassic (see Weissert and Mohr, 1996). A prominent negative carbon isotope pulse in the Oxfordian Transversarium ammonite zone and a second less pronounced one in the Bifurcatus ammonite zone document an extraordinary carbon-12 enrichment of the marine carbon reservoir within only a few tens of thousand to hundred thousand years. Padden et al. (2001) compared the first of these two anomalies with the well documented negative carbon-isotope anomaly at the Paleocene-Eocene boundary (Dickens et al., 1995). Dickens and his colleagues calculated that only a sudden influx of methane

derived from sub-seafloor sources can explain the observed carbon-isotope pattern. Methane is extremely enriched in the light carbon isotope. It is stored in sedimentary gas hydrates consisting of solid water-methane crystals and stable under a wide range of subseafloor temperatures and pressures. Sudden methane release could have resulted from deep water warming. Padden et al (2001) suggest that oceanographic circulation changes following the first significant Tethyan-Atlantic connection with the Pacific could have resulted in Pacific deep water warming and destabilization of gas hydrates.

The Tithonian segment of the C-isotope curve is marked by a long term trend to lighter carbon isotope values reaching low values of about 1‰ near the Jurassic-Cretaceous boundary. The trend coincided with decreasing organic carbon sedimentation and with the first episode of widespread nannofossil ooze deposition in pelagic environments (Weissert and Channell, 1989). Conditions favouring the expansion of carbonate sedimentation into pelagic environments include a sea level drop coupled with a lowering of the CCD and increasing weathering rates as recorded in a trend to heavier Sr-isotope values (Jones and Jenkyns, 2001).

7. Conclusions

The comparison of carbon-isotope stratigraphy from the Helvetic nappes with well-dated sections in the Jura Mountains, the Southern Alps and the Vocontian Basin revealed several key 'tie-points' in the Late Jurassic $\delta^{13}\text{C}$ curve which can be used for stratigraphic correlation. A negative excursion in the Oxfordian Transversarium ammonite zone is well-dated at both Auenstein, in the Jura Mountains and at Vergons, in the Vocontian Basin. A second negative $\delta^{13}\text{C}$ excursion, in the Bifurcatus ammonite zone, is dated at the Auenstein section. The positive $\delta^{13}\text{C}$ values in Late Oxfordian, which are bracketed by these negative excursions, have also been reported in other sections (Scholle & Arthur 1980; Jenkyns 1996; Bartolini et al. 1999). A Late Kimmeridgian positive $\delta^{13}\text{C}$ excursion is dated in the Helvetic nappe sections (Weissert & Mohr 1996; this study). The final distinctive feature of the Late Jurassic $\delta^{13}\text{C}$ curve is the relatively smooth shift to depleted values towards the Jurassic/Cretaceous boundary which is well-dated in the Southern Alpine sections (Weissert & Channell 1989). The presented carbon-isotope stratigraphy improves the chronological control of the carbonate successions of the Helvetic and Ultrahelvetic nappes and it will provide a robust framework for future investigations of paleoceanographic change in the alpine Tethys. The new carbon isotope curve records two negative carbon isotope pulses which may be explained by a sudden enrichment of the marine carbon reservoir with methane-derived light ^{12}C (Padden et al. 2001). The positive carbon isotope anomalies identified in the Late Oxfordian and in the Late Kimmeridgian are smaller in amplitude than the Cretaceous carbon isotope excursions. This indicates that the Late Jurassic carbon cycle was more stable than the Cretaceous one.

Acknowledgements

This project was supported by the Swiss Science Foundation and by ETH Zürich. We are grateful to Stefano Bernasconi for his continuous and kind support in the Stable Isotope Lab. We thank Karl Föllmi and Hugh Jenkyns for their helpful reviews of an earlier version of this manuscript.

REFERENCES

- ALLENBACH, R.P., 2001: Synsedimentary tectonics in an epicontinental sea: a new interpretation of Oxfordian basins of northern Switzerland. *Eclogae Geol. Helv.*, 94, 265–288.
- ARTHUR, M.A., DEAN, W.E., SCHLANGER, S.O., 1985: Variations in the global carbon cycle during the Cretaceous related to climate, volcanism and changes in atmospheric CO₂. In: *The Carbon Cycle and Atmospheric CO₂: Natural Variations Archaean to the Present* (Ed. by SUNDQUIST, E.T.S. & BROECKER, W.E.). Geophysical Monograph 32, 504–530.
- BARTOLINI, A., BAUMGARTNER, P.O. & GUEX, J. 1999: Middle and Late Jurassic radiolarian palaeoecology versus carbon-isotope stratigraphy. *Palaeogeography, Palaeoclimatology, Palaeoecology* 145, 43–60.
- BILL, M., BAUMGARTNER, P.O., HUNZIKER, J.C. & SHARP, Z.D. 1995: Carbon isotope stratigraphy of the Liesberg Beds Member (Oxfordian, Swiss Jura) using echinoids and crinoids. *Eclogae Geol. Helv.* 88, 135–155.
- CASATI, P. & TOMAI, M. 1969: Il giurassico ed il cretaceo del versante settentrionale del Vallone Bellunese e del gruppo del M. Brandol. *Riv. ital. Paleontologia e Stratigrafia* 75, 206–316.
- CHANNELL, J.E.T. & GRANDESSO, P. 1987: A revised correlation of Mesozoic polarity chrons and calpionellid zones: Earth and Planetary Sci. Letters 85, 222–240.
- CHANNELL, J.E.T., BRALOWER, T.J. & GRANDESSO, P. 1987: Biostratigraphic correlation of Mesozoic polarity chrons CM1 to CM23 at Capriolo and Xausa (Southern Alps, Italy). *Earth and Planetary Sci. Letters* 85, 203–221.
- DE RAFELIS, M., 2000: Apport de l'étude de la spéciation du manganèse dans les carbonates pélagiques à la compréhension du contrôle des séquences eustatiques de 3ème ordre [unpublished Ph.D. thesis], Université Pierre et Marie Curie, Paris, 214 pp.
- DE RAFELIS, M., EMMANUEL, L., RENARD, M., ATROPS, F., DU CHENE, J.R. 2001: Geochemical characterization (Mn content) of third order eustatic sequences in Upper Jurassic pelagic carbonates of the Vocontian Trough. *Eclogae Geol. Helv.*, 94, 145–152.
- DICKENS, G.R., O. NEIL, J.R., REA, D.K. & OWEN, R.M., 1995: Dissociation of oceanic methane hydrate as a cause of the carbon isotope excursion at the end of the Paleocene: *Paleoceanography*, 10, 965–971.
- FERRERI, V., WEISSERT, H., D'ARGENIO & BUONOCUNTO, P. 1997: Carbon-isotope stratigraphy: A tool for basin to carbonate platform correlation: *Terra Nova* 9, 57–61.
- FRÜH-GREEN, G.L., WEISSERT, H. & BERNOULLI, D. 1990: A multiple fluid history recorded in Alpine ophiolites: *J. Geol. Soc London* 147, 959–970.
- FUNK, H., FÖLLMI, K.B. & MOHR, H. 1993: Evolution of the Tithonian-Aptian carbonate platform along the northern Tethyan margin, eastern Helvetic Alps. In: *Cretaceous carbonate platform* (Ed. by Simo, J.A.T., Scott, R.W. & Masse, J.P.). *Amer. Assoc. Petrol. Geol. Memoir* 56, 387–407.
- GANSNER, C. 2000. *Geologische Untersuchungen im Gebiet Gemmipass – Lämmernalp – Kummern, Leukerbad, Kanton Wallis* [unpublished Diploma thesis]: ETH Zürich, Zürich, 138 pp.
- GRADSTEIN, F.M. & OGG, J. 1996: A Phanerozoic time scale. *Episodes* 19, 3–5.
- GUILLAUME, H. 1957: *Géologie du Montsalvens (Préalpes fribourgeoises)*. [unpublished Ph.D. thesis] Université de Fribourg, 171 pp.
- GYGI, R.A. 1969: Zur Stratigraphie der Oxford-Stufe (oberes Jura-System) der Nordschweiz und des süddeutschen Grenzgebietes. *Beitr. Geol. Karte Schweiz* 139.
- GYGI, R.A. 2000a: Integrated Stratigraphy of the Oxfordian and Kimmeridgian (Late Jurassic) in northern Switzerland and adjacent southern Germany. *Mem. Swiss Acad. Sci.* 104, Basel, Birkhäuser, 152 pp.
- GYGI, R.A. 2000b: Zone boundaries and subzones of the Transversarium Ammonite Zone (Oxfordian, Late Jurassic) in the reference section of the zone, northern Switzerland. In: *Advances in Jurassic research 2000; Proc. fifth international symp. Jurassic system*. (Ed. by HALL RUSSELL, L. & SMITH PAUL, L.) *GeoResearch Forum: Zurich, Switzerland, Trans Tech Publ.* 77–84.
- GYGI, R.A. & PERSOZ, F. 1987: Mineralostratigraphy, litho- and biostatigraphy combined in correlation of the Oxfordian (Late Jurassic) formations of the Swiss Jura range. *Eclogae Geol. Helv.* 79, 385–454.
- HUMPHREY, J.D., RANSOM, K.L. & MATTHEWS, R.K. 1986. Early meteoric diagenetic control of upper Smackover production, Oaks Field, Louisiana. *Amer. Assoc. Petrol. Geologists Bull.* 70, 70–85.
- JAN DU CHENE, R., ATROPS, F., EMMANUEL, L., DE RAFELIS, M. & RENARD, M. 2000: Palynology and sequence stratigraphy in the Tethyan Upper Oxfordian – Lower Kimmeridgian, S-E France. *Bull. Centre de Rech. Exploration Production Elf – Aquitaine* 22/2, 273–321.
- JENKYN, H.C. 1996: Relative sea-level change and carbon isotopes: data from the Upper Jurassic (Oxfordian) of central and southern Europe. *Terra Nova* 8, 75–85.
- JENKYN, H.C., GALE, A.S. & CORFIELD, R.M. 1994: Carbon- and oxygen-isotope stratigraphy of the English Chalk and Italian Scaglia and its palaeoclimatic significance. *Geol. Magazine* 131, 1–34.
- JONES, C.E. & JENKYN, H.C., 2001: Seawater strontium isotopes, oceanic anoxic events and seafloor hydrothermal activity in the Jurassic and Cretaceous. *Am. J. of Science*, 301, 112–149.
- KUGLER, C. 1987: Die Wildegg-Formation im Ostjura und die Schilt-Formation im östlichen Helvetikum: ein Vergleich. *Mitt. Geol. Inst. ETH und Univ. Zürich, N.F.* 259, 209 p.
- KUHN, O. 1996: Der Einfluss von Verwitterung auf die Paläozoographie zu Beginn des Kreide-Treibhausklimas (Valanginian und Hauterivian) in der West-Tethys. [unpublished Ph.D. thesis]: ETH Zürich, Switzerland, 380 pp.
- LETOLLE, R., RENARD, M., BOURBON, M., FILLY, A., BENSON, W.E., SHRIDAN, R.E., PASTOURET, L., ENOS, P., FREEMAN, T., MURDMAA, I.O., GRADSTEIN, F., SCHMIDT, R.R., WEAVER, F.M. & STUERMER, D.H. 1978: ¹⁸O and ¹³C isotopes in Leg 44 carbonates: a comparison with the Alpine series. In: *Initial Reports of the Deep Sea Drilling Project* (Ed. by WORSTEL, P.): College Station, TX, United States, Ocean Drilling Program 44, p. 567–573.
- MATTER, A., DOUGLAS, R.G. & PERCH-NIELSEN, K. 1975: Fossil preservation, geochemistry, and diagenesis of pelagic carbonates from Shatsky Rise, Northwest Pacific. In: *Initial Reports of the Deep Sea Drilling Project*, (Ed by MOBERLY, R.) College Station, TX, United States, Ocean Drilling Program 32, 891–921.
- MENEGATTI, A.P., WEISSERT, H., BROWN, R.S., TYSON, R.V., FARRIMOND, P., STRASSER, A. & CARON, M. 1998: High-resolution δ¹³C stratigraphy through the early Aptian “Livello Selli” of the Alpine Tethys. *Paleoceanography* 13, 530–545.
- MOHR, H.M. 1992: Der helvetische Schelf der Ostschweiz am Übergang vom späten Jura zur frühen Kreide. [unpublished Ph.D. thesis] ETH Zürich, 221 pp.
- PADDEN, M., WEISSERT, H. & DE RAFELIS, M. 2001: Evidence for Late Jurassic release of methane from gas hydrate. *Geology* 29, 223–226.
- ROD, E. 1937: *Stratigraphie des Malm der Graustock Hutstock Gruppe (Melchtal, Kt. Obwalden)*. [unpublished Ph.D. thesis]: Universität Bern, Bern, 56 pp.
- SCHNEIDER, S. 1998: *Sedimentologie des helvetischen Dogger und Malm sowie C-Isotopenstratigraphie des Quintnerkalks im Gebiet der Melchsee-Frutt*. [unpublished Diplom thesis], ETH, Zürich, 107 pp.
- SCHOLLE, P. & ARTHUR, M.A. 1980: Carbon isotopic fluctuations in pelagic limestones: Potential stratigraphic and petroleum exploration tool. *Amer. Assoc. Petrol. Geol. Bull.* 64, 67–87.
- SHARMA, T. & CLAYTON, R.N. 1965: Measurement of 0–18/0–16 ratios of total oxygen of carbonates. *Geochimica et Cosmochimica Acta* 29, 1347–1353.

- WEISSERT, H.J. 1979: Die Paleozeanographie der südwestlichen Tethys in der Unterkreide. Mitt. geol. Inst. ETH u. Univ. Zürich, NF 226, 174 pp.
- WEISSERT, H. & CHANNELL, J.E.T. 1989: Tethyan carbonate carbon isotope stratigraphy across the Jurassic-Cretaceous boundary: an indicator of decelerated carbon cycling. *Paleoceanography* 4, 483–494.
- WEISSERT, H. & LINI, A. 1991: Ice Age interludes during the time of Cretaceous greenhouse climate? In: *Controversies in Modern Geology* (Ed by MÜLLER D.W., MCKENZIE J.A. & WEISSERT H.), Academic Press, 173–191.
- WEISSERT, H. & MOHR, H. 1996: Late Jurassic climate and its impact on carbon cycling: *Palaeogeography, Palaeoclimatology, Palaeoecology* 122, 27–43.
- WISSLER, L., WEISSERT, H., MENEGATTI, A., FERRERI, V., B., D.A., BUONOCUNTO, F., RASPINI, A. & AMMODIO, S. 1999: ^{13}C -stratigraphy in Barremian-Aptian shallow water carbonates of southern Italy. *Abstr. Europ. Union Geosci. Conf.; EUG 10*, March 28–April 1, 1999., p. 218.
- ZIEGLER, P. 1988: Evolution of the Arctic North Atlantic and the western Tethys: *Am. Ass. Petroleum Geol. Memoir* 43, 198p.

Manuscript received December 24, 2001

Revision accepted August 31, 2002